Available online at www.sciencedirect.com

SciVerse ScienceDirect

Procedia CIRP 4 (2012) 73 – 78

www.elsevier.com/locate/procedia

3rd CIRP Conference on Process Machine Interactions (3rd PMI)

Modeling of the Thermomechanical Process Effects on Machine Tool Structures

Tobias Maier[a]*, Michael F. Zaeh[a]

[a]*Institute of Machine Tools and Industrial Management (iwb), Technische Universität München, Boltzmannstraße 15, Garching 85748, Germany*
* Corresponding author. Tel.: +49-89-289-15483; fax: +49-89-289-15555. *E-mail address*: tobias.maier@iwb.tum.de.

Abstract

Thermally induced deviations are a key issue in the development of machine tools, especially when considering the actual trends of high performance and dry cutting. The interactions between the cutting process and the machine tool structure are significant boundary conditions for the numerical prediction of the thermomechanical machine behavior. Within this paper an approach for the holistic modeling of process effects is presented, including process heat, cutting forces and increased load on feed and main drives. The modeling approach is supported by experimental investigations on a lathe to provide empiric data for the link between cutting forces and active drive power.

Keywords: thermomechanical process machine interactions; finite element analysis; process effect model; elctrical drive power ; cutting forces

1. Introduction

The accuracy of machine tools is mainly limited by thermally induced deviations. This effect is of increasing importance, especially considering the actual trends of high performance and dry cutting. The thermo-mechanical machine behavior is strongly influenced by inner heat sources and environmental effects. Being subject to interactions with the machine tool structure and the machining task, the cutting process plays a leading role for the thermally induced deviations. Thereby, the process effects on the machine tool have to be considered from a holistic point of view, including the heat input, the cutting forces and the additional loads on the main and feed drives.

Regarding the complexity and number of influences, the determination of the thermomechanical machine tool behavior is highly challenging. The finite element analysis (FEA) is an approved numerical method for the approximated solution of mechanical and thermal structural problems [1, 2, 3, 4, 5]. The determination of thermomechanical deviations is carried out in two steps. The thermal solver calculates a temperature distribution based on the discretized Fourier differential equation. Subsequently the heat expansion coefficients in the mechanical model lead to thermally induced deviations. This procedure can be performed for the entire time range or within each time step (quasi-coupled solution). The accuracy of the temperature calculation is strongly dependent on the definition of the boundary conditions. These can be convective or emissive terms (e. g. for ambient conditions), temperature values or heat fluxes (i. e. for heat sources) [6].

The cutting process plays a key role for the thermal machine behavior and therefore is a critical part for the definition of boundary conditions. However, existing approaches mostly consider only individual effects like the cutting heat for the application in finite element models [5]. In order to achieve an appropriate representation of the process, this paper shows an integral modeling approach of the process impact that is incorporating all relevant process effects for thermal finite element analyses of machine tools. The work focuses a turning process and its influence on the structure of a lathe.

Therefore, an approach for the holistic process modeling is developed. The process model includes

2212-8271 © 2012 The Authors. Published by Elsevier B.V. Selection and/or peer-review under responsibility of Prof. Eiji Shamoto
Open access under CC BY-NC-ND license. doi:10.1016/j.procir.2012.10.014

multiple modules for the description of the particular interactions with the machining task or the structure. The process heat and the cutting forces are calculated on the basis of empiric relations. Using existing approaches, the process model is supported by substantial experimental investigations made on a lathe. The determined cutting forces are significant inputs for the drive module. Based on the operating position and the geometry of the machine, the resulting loads on elements like the bearings, the ball screw drives, or the electric drives are derived. The paper will thereby focus the impact from cutting forces and the drive module. The resulting heat fluxes and heat impact zones can directly be used in thermal FEA of machine tools.

The experimental work in this paper provides empiric data supporting the modeling of forces and power and is done on a 3-axis lathe (Spinner TC 600, cf. Fig. 1). The lathe is equipped with a motorized spindle (1), three feed drives for x- (2), y- (3) and z-direction (4) as well as a tool changer (5). Drives in y-direction are performed by a combined motion of the x- and y-feed drive.

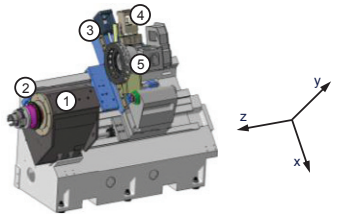

Fig. 1. Model of the lathe used for experimental investigations

2. Modeling of boundary conditions

2.1. Boundary condition model

A numerical approach for the prediction of thermally induced deviations is always dependent on the modeling quality of boundary conditions. The machine tool structure is influenced by environmental impact, such as a change of ambient temperature, and internal heat sources, such as feed drives or the cutting process. The internal heat impact can be classified as dependent or independent of the machining task. Independent heat sources are mostly aggregates like control cabinets that have continuous heat losses. These can be modeled by constant heat fluxes into the machine tool structure. The description of the task dependent heat sources is by far more complex with the heat fluxes being time dependent (and in certain cases at moving positions). Fig. 2 shows a thermal effect chain that leads to heat impact into the machine tool. Based on the numerical control (NC) program, the machine tool's kinematics define movements of the machine specific axes as well as the rotational speed of the main spindle. On the one hand, these movements are an important input for the modeling of the drive systems with the velocity determining the heat loss in mechanical components, such as bearings. On the other hand, they are the basis for the behavior of the cutting process. Latter is essential for the determination of the thermal boundary conditions. First, the cutting heat is transferred into the work piece, the tool and the chips, which leads to a heat impact on the machine tool structure. Second, the cutting process is indirectly influencing the boundary conditions with the resulting cutting forces significantly increasing the load on the drives and bearings.

The heat sources as well as the ambience determine a time dependent temperature field and, in combination with thermal expansion coefficients, are subsequently leading to thermally induced deviations. The latter eventually are limiting the machining accuracy. Additionally, these deviations have an impact on the process and drive system input as they are distorting the real positions. Concerning the bearings, they can even lead to higher loads and therefore heat losses.

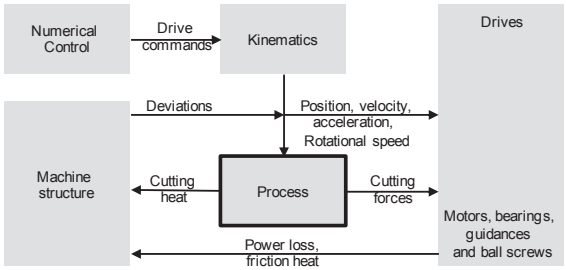

Fig. 2. Machining task dependent heat sources in machine tools

2.2. Cutting force model

The modeling of thermal boundary conditions requires static mean values for the cutting process forces. Thus, the calculation can be done using the well-proven relations of KIENZLE & VICTOR [7, 8]. As there are correction factors and data for the most common materials, processes and parameters those empiric equations provide good predictability for static cutting and feed forces.

The cutting force F_C can be calculated from the width of cut b, the thickness of cut h, the main value of the specific cutting force $k_{C1.1}$ and the rising parameter of the specific cutting force $1\text{-}m_C$ as follows:

$$F_C = b \cdot h^{1-m_C} \cdot k_{C1.1} \qquad (1)$$

The tool cutting edge angle κ defines b and h from the depth of cut a_p and the feed rate f:

$$b = \frac{a_p}{\sin\kappa}, \qquad h = f \cdot \sin\kappa \qquad (2)$$

The determination of the feed force F_F can be done in an analog way using the specific feed force $k_{f1.1}$:

$$F_F = b \cdot h^{1-m_F} \cdot k_{F1.1} \quad (4)$$

These equations provide a basis for the calculation of boundary conditions for thermal machine tool simulations.

2.3. Cutting heat model

The cutting heat model is based on the empiric cutting force model and benefits from the fact that nearly the entire cutting energy is transformed into heat [8]. The active process power P_A is the sum of the cutting power P_C and the feed power P_F:

$$P_A = P_C + P_F \quad (4)$$

The cutting power can be calculated as product of cutting force F_C and cutting speed v_C, the feed power as product of feed force F_F and feed rate v_F. Assuming that the active process power is approximately equal to the heat impact, it is possible to determine the heat sources. For steel it is widely acknowledged that the cutting heat is roughly divided into three parts:

- 75 % of the heat is carried away by the chips,
- 18 % of the heat goes into the tool and
- 7 % of the heat is affecting the work piece.

Thus, an estimated modeling of the cutting heat is possible with respect to a thermal machine tool simulation.

2.4. Drive module

The drive model defines how to calculate the electric power and heat loss from the kinematics' output and the cutting forces. Fig. 3 shows the relevant thermal aspects of a generic feed axis.

Inputs are the position x, the velocity v, the acceleration a and the cutting force F_C. Starting with the cutting force, there are several effects inside the axis which affect the actual force that has to be delivered by the motor. Inertia forces have to be added or subtracted when accelerating or decelerating the axis. Based on the machine tool's geometry several axes can be subject to gravity effects, like the x- and y-axis of the examined lathe. The downhill-slope force therefore effects all motions of those axes and cannot be ignored (cf. section 4.1). The velocity and the resulting force are the important inputs for the calculation of friction in the guideways, the bearings and the ball screw, which leads to a direct heat impact on the machine tool structure. Additionally, this friction increases the load on the drive motor. Subsequently, the final motor load as well as the degree of efficiency determine the heat impact from the motor. Regarding the main drive the approach is quite similar, except for the friction from guideways and ball screw as well as the gravity effects can be ignored.

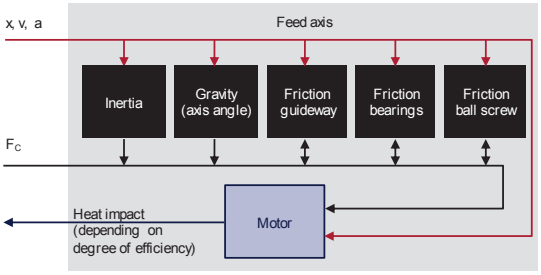

Fig. 3. Relevant thermal aspects of a generic feed axis

3. Experimental setup

The modeling of thermal boundary conditions is supported by experimental investigations. The paper will focus on cutting forces as well as main and feed drive power. The determination of the distribution of cutting heat into the work piece, the tool and the chips is currently planned. The aim of these investigations is to get a direct link between the cutting parameters, forces, heat and especially the necessary electrical power. Only this direct link can assure a holistic view on the machining task dependent boundary conditions.

The measurements provide data for chosen parameter sets for longitudinal and for face turning and cover different machining conditions as follows:

- Idle running of feed and main drives at different velocities
- Varying depths of cut a_p from *0.5* to *1.5 mm*
- Varying feed rates f from *0.1* to *0.3 mm/rotation*
- Varying cutting speeds v_C from *120* to *180 m/min*

All experimental investigations were done with a lathe tool with changeable cutting plates of type DC-T, probes of C45E steel (1.1191) with an original diameter of *45 mm* and using constant cutting speeds within each parameter test.

3.1. Cutting forces

In order to measure the cutting forces, the lathe was equipped with a 3-axes dynamometer (Kistler type 9121 for lathes), mounted on the tool holder. This allows the simultaneous acquisition of cutting, feed and passive forces. Fig. 4 shows an exemplary force diagram for longitudinal turning.

Regarding the first *0.3 s* it can be seen that the cutting forces increase until reaching an approximately constant value. The data is subsequently processed to determine a mean value within the constant range of the force trend.

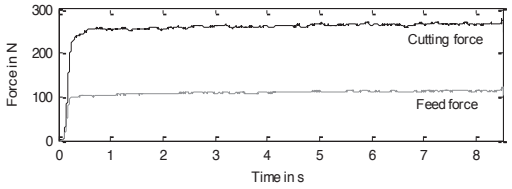

Fig. 4. Exemplary smoothed cutting force diagram for longitudinal turning (parameters: $a_p = 0.5$ *mm*, $f = 0.2$ *mm/rotation*, $v_C = 150$ *m/min*)

An analog chart for face turning can be found in Fig. 5. Aside from the similar starting and constant sections, it can be clearly seen that the cutting forces increase at the end of the test. This is resulting from the rotational speed limit that was defined by the lathe and the used jaw chuck (*2000 rotations/min*). With decreasing diameter (time range from *2.5* to *4 s*) the constant cutting speed can not longer be guaranteed which leads to rising cutting forces. Consequently, only the constant section of the force trend was used for the following data processing.

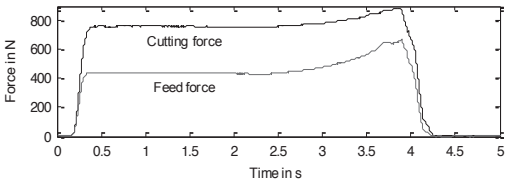

Fig. 5. Exemplary smoothed cutting force diagram for face turning (parameters: $a_p = 1.5$ *mm*, $f = 0.2$ *mm/rotation*, $v_C = 150$ *m/min*)

3.2. Electrical drive power

The experimental investigation of the electrical power in feed and main drives is more complex. Power measurements for the whole machine tool are benefitting from the fact that most power analyzers are designed to work at net frequencies of *50* or *60 Hz*. As the central power supply represents the usage of all drives and aggregates combined, this does not seem appropriate for the analysis of the process effects on single drives. Therefore, it is necessary to measure the electrical power between the intermediate direct current link and the drive motor itself. The current and the pulse width modulated voltage of all three phases were simultaneously recorded by current clamps (Tektronix A6303) and differential probes (Testec TT-SI 9002) attached to an oscilloscope (Yokogawa DL 708E) sampling with *100 kHz*. Fig. 6 (left) shows an exemplary voltage chart for a short time range, clearly indicating that the pulses are sampled with sufficient resolution. The resulting voltage causes a sinusoidal current trend which is presented in Fig. 6 (right).

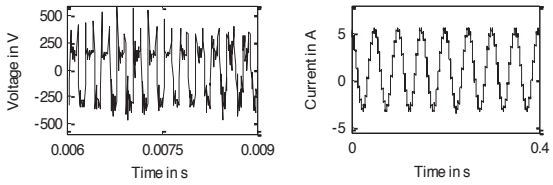

Fig. 6. Exemplary voltage chart, showing the pulse duration modulation and exemplary current chart, resulting from the voltage

As both signals are recorded in high resolution it is possible to calculate the active electrical power as product of voltage and current and subsequently the active energy, as can be seen exemplarily in Fig. 7. The energy chart is useful for the calculation of mean power values as it shows wether the active power is constant over the examined time range.

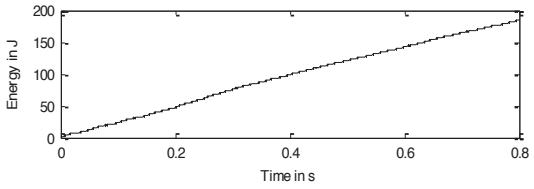

Fig. 7. Exemplary active electrical energy, indicating near constant power for the examined time range

4. Results

4.1. Idle running of feed and main drive

In a first step the feed and main drives were examined while running idle, delivering a basis for the following investigations of the process charged drives. The x-axis feed drive behavior is of special interest as it is charged by an axis that is subject to gravitation (cf. Fig. 1). Fig. 8 shows the active power resulting from a rapid traverse motion in x-direction. The first peak results from the downward drive, the second from the upward drive. It can be clearly seen that the influence of gravitation (see section 2.4) cannot be neglected. Fig. 9 shows the dependency of the main spindle's active power on the rotational speed. It can be seen that a linear behavior cannot be assumed over the complete speed range.

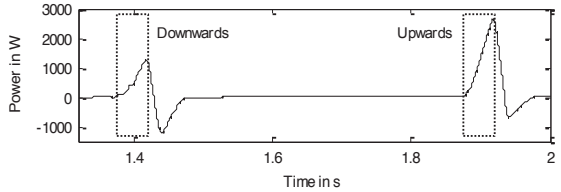

Fig. 8. Active power of the x-feed drive for a rapid travers motion in x-direction (first downwards, second upwards)

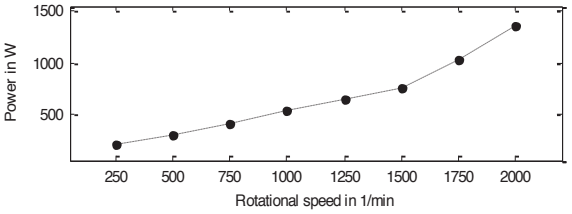

Fig. 9. Active power of the main spindle for idle running at different rotational speeds

4.2. Longitudinal turning

When considering the additional loads of the drives due to process forces, the cutting and the feed forces are of highest interest as they have to be provided by the main and feed drives. For longitudinal turning the additional feed power is linked to the z-feed drive, the cutting power to the main spindle. Fig. 10 presents the process forces as well as the active power of the main and the z-feed drive for different cutting parameters.

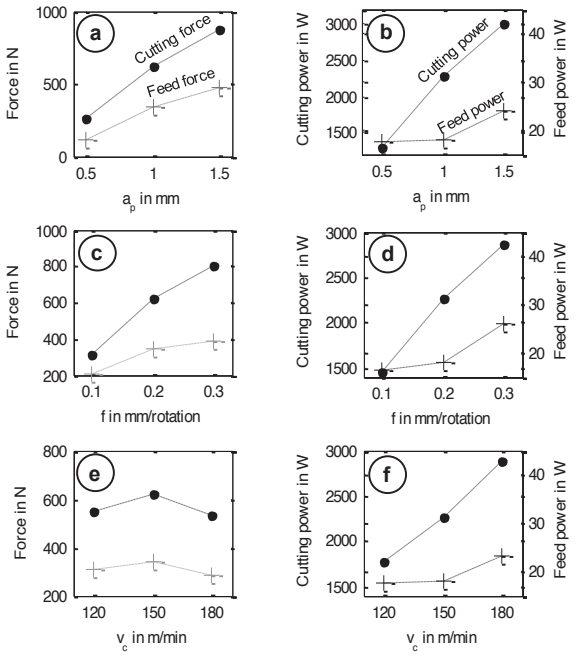

Fig. 10. Process forces (a) as well as active power (b) of main and z-feed drives for different depths of cut ($f = 0.2$ *mm/rotation*, $v_C = 150$ *m/min*); process forces (c) as well as active power (d) of main and z-feed drives for different feed rates ($a_p = 1$ *mm*, $v_C = 150$ *m/min*); process forces (e) as well as active power (f) of main and z-feed drives for different cutting speeds ($a_p = 1$ *mm*, $f = 0.2$ *mm/rotation*)

The charts show the behavior predicted by the equations in section 2.2 like the approximately linear relation between cutting force and depth of cut. The active power of both drives is nearly proportional to the force trends with the cutting power being significantly higher than the feed power, which is a typical phenomenon for turning processes. Regarding Fig. 10 (e) and (f) the relation between cutting force and power seems different. This results from the increasing cutting speed which is also affecting the cutting power.

4.3. Face turning

In contrast to the longitudinal turning the feed motion for the face turning process is performed by the x-axis feed drive. The x-axis on the examined lathe is subject to gravity effects as it is sloped. This leads to complex resulting loads on the drive motor as presented in section 2.3. Fig. 11 shows the forces and the active power of the x-feed drive. While the measured forces reflect the predicted behavior, the active power shows quite different trends. The negative power values indicate that the motor is recuperating energy. This effect results from the gravity load on the x-axis. However, the process parameters are influencing this value as well. The increasing cutting force over the depth of cut leads to a decrease of recuperation. Higher feed rates and cutting speeds are leading to a higher axis velocity, and therefore to an increasing recuperation. This complex behavior shows the need for a detailed thermal modeling of the drive systems.

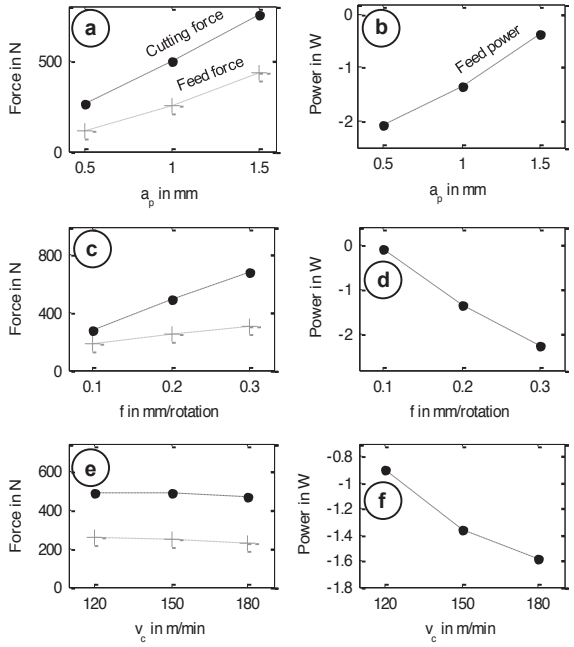

Fig. 11. Process forces (a) as well as active power (b) of the x-feed drive for different depths of cut ($f = 0.2$ *mm/rotation*, $v_C = 150$ *m/min*); process forces (c) as well as active power (d) of the x-feed drive for different feed rates ($a_p = 1$ *mm*, $v_C = 150$ *m/min*); process forces (e) as well as active power (f) of the x-feed drive for different cutting speeds ($a_p = 1$ *mm*, $f = 0.2$ *mm/rotation*)

Concerning face turning, the main spindle is accelerating during the feed motion as it is providing a constant cutting speed over a decreasing diameter. Mean power values are therefore not significant. Fig. 12 shows the transient active power of the main drive for different feeds. Similar measurements were performed for varying depths of cut and cutting speeds. Expectedly, the power shows a disproportionately high increase for rising feed rates. This results from the rotational speed to power relation in Fig. 9.

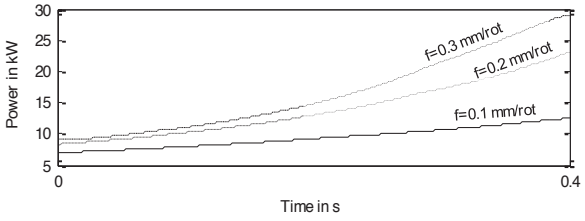

Fig. 12. Active power of the main drive for different feeds

The experimental results show that the existing equations are appropriate for the cutting force calculation for the use in thermal boundary condition modeling. The link between forces and electrical power provides empirical fitting data for the drive modeling.

4.4. FE analysis for different parameters

Boundary conditions that are calculated by the approach of section 2 and supported by the empiric results of chapter 4 are directly usable for thermal FEA. For the lathe a FE model is existing, build from volume and shell elements (ca. 290000 elements total) and capable for thermal and mechanical calculations. All relevant surfaces are loaded by film coefficients to represent convection and emission to the ambience.

While other thermal effects (like cooling or friction of bearings) are ignored, the model of the lathe is loaded with heat fluxes for feed and main drives, representing the process parameters (feed rates of *0.1* and *0.3 mm/rotation* (a_p = *1 mm*, v_C = *150 m/min*)) as well as a couple of traverse motions of the feed drives. The simulation is performed by serial processing, so at first a temperature distribution is calculated from heat fluxes as well as ambient boundary conditions. On this basis the thermally induced deviations of the machine tool structure is simulated.

Fig. 13 shows the transient relative displacement results between tool and work piece (normalized to the maximum due to confidentiality reasons) of the FE simulation. The chart shows clear differences between both parameter sets, indicating the importance of the integral process effect modeling.

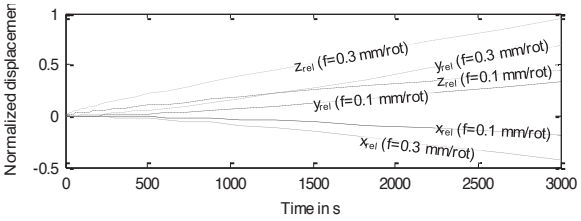

Fig. 13. Thermomechanical relative displacements between tool and workpiece, simulated through a FEA for two different cutting parameter sets

5. Conclusions and perspectives

Within this paper an approach for the holistic modeling of thermal boundary conditions due to process effects is presented. The experimental investigations provide empiric data for the link of cutting forces and power and subsequently the heat loss. Thus, the basis for thermal FEA of machine tools is extended to include the cutting process with the relevant effects.

Investigations in the near future will reveal wether the cutting heat modeling as presented here is a good approximation. Therefore, temperature measurements of tool, work piece and chips are planned.

Acknowledgements

The authors extend their sincerest gratitude to the German Research Foundation (DFG) for its generous support.

References

[1] Weck, M., Wundram, K., 1998. Verbesserung der Genauigkeit thermischer Simulationen von Maschinenelementen und Baugruppen. Konstruktion 50 (1998) 7/8, pp. 26 – 30.

[2] Weidermann, F., Nestmann, S., 2000. Simulation und Optimierung des thermischen Verhaltens von Werkzeug-maschinenkomponenten. 1. Dresdner WZM-Fachseminar: Thermik an Werkzeugmaschinen. Dresden, November 30 and December 1.

[3] Kim, J.-J., Jeong, Y. H., Cho, D.-W., 2004. Thermal behaviour of a machine tool equipped with linear motors. International Journal of Machine Tools & Manufacture 44 (2004), pp. 749 – 758.

[4] Zhao, H., Jianguo, Y., Jinhua, S., 2007. Simulation of thermal behavior of a CNC machine tool spindle. International Journal of Machine Tools & Manufacture 47 (2007), pp. 1003 – 1010.

[5] Gleich, S., 2008. Simulation des thermischen Verhalten spanender Werkzeugmaschinen in der Entwurfsphase. Verlag Wissenschaftliche Scripten, Chemnitz (doctoral thesis).

[6] Zaeh, M. F., Maier, T., 2010. Finite Element Analysis for Thermal Behavior, in: *"Thermal Deformation in Machine Tools"* Ito, Y., Editor. McGraw-Hill, New York, pp. 143 – 147.

[7] Kienzle, O.; Victor, H., 1952. Die Bestimmung von Kräften und Leistungen an spanenden Werkzeugmaschinen. VDI-Z 94 (1952) 11 – 12, pp. 155 – 171.

[8] König, W., 1984. Fertigungsverfahren Band 1. VDI-Verlag, Düsseldorf.